

# Face Images Database Indexing for Person Identification Problem

## Jyotirmay Dewangan

*M. Tech Student, School of Information Technology  
Indian Institute of Technology Kharagpur  
Kharagpur, 721302, India*

*jyotirmay.sg@gmail.com*

## Somnath Dey

*Faculty, Department of Computer Science and Engineering  
Indian Institute of Technology Indore  
Indore, 453441, India*

*somnathd@iiti.ac.in*

## Debasis Samanta

*Faculty, School of Information Technology  
Indian Institute of Technology Kharagpur  
Kharagpur, 721302, India*

*dsamanta@iitkgp.ac.in*

---

## Abstract

Face biometric data are with high dimensional features and hence, traditional searching techniques are not applicable to retrieve them. As a consequence, it is an issue to identify a person with face data from a large pool of face database in real-time. This paper addresses this issue and proposes an indexing technique to narrow down the search space. We create a two level index space based on the SURF key points and divide the index space into a number of cells. We define a set of hash functions to store the SURF descriptors of a face image into the cell. The SURF descriptors within an index cell are stored into kd-tree. A candidate set is retrieved from the index space by applying the same hash functions on the query key points and kd-tree based nearest neighbor searching. Finally, we rank the retrieved candidates according to their occurrences. We have done our experiment with three popular face databases namely, FERET, FRGC and CalTech face databases and achieved 95.57%, 97.00% and 92.31% hit rate with 7.90%, 12.55% and 23.72% penetration rate for FERET, FRGC and CalTech databases, respectively. The hit rate increases to 97.78%, 99.36% and 100% for FERET, FRGC and CalTech databases, respectively when we consider top fifty ranks. Further, in our proposed approach, it is possible to retrieve a set of face templates similar with query template in the order of milliseconds. From the experimental results we can substantiate that application of indexing using hash function on SURF key points is effective for fast and accurate face image retrieval.

**Keywords:** Biometric, Face Identification, Biometric-data Indexing, SURF, Index Key Generation.

---

## 1. INTRODUCTION

Of late, biometric-based person authentication system is gaining importance due to its wide spread applications such as personal identification [1], PDA, smart card [2, 3], access control [4, 5], surveillance [6], forensic applications [1, 7, 8], biometric passports [5, 9, 10], national identity card registration [11, 12, 13] and human computer interaction, etc. [1]. In these applications, there is a need to deal with large-scale databases [11, 14]. For example, Unique Identification Authority of India [11, 14] has planned to register 600 million users in India in next few years where the number of accesses per day (in different public and private domains) are expected to be around 1 to 5 million.

The major concern in the face identification is high dimensional feature vector. In a large-scale biometric system, exhaustive searching in face database to retrieve an identity is typically slow

and may not be acceptable. Also, the false acceptance error grows with the size of database [15]. As a consequence, the response time, search and retrieval efficiency are affected in addition to the accuracy of the system.

However, the current state-of-the-art research [24, 25, 26] in face recognition is mainly focused to solve the problem of variable lighting, pose, facial expression and aging in verification mode. The Face Recognition Grand Challenge (FRGC) [44, 45] shows a large improvement on face recognition accuracy for large number of face images with different lighting conditions, illuminations, poses and expressions. There are very few works [28, 29, 30] which addressed the problem of identification of a face image in large database. Though, some work [16, 17, 18, 19, 20, 21, 22, 23, 24, 25, 26] tried to alleviate the limitations of identification by proposing the dimensionality reduction techniques. But they use linear searching or nearest neighbor searching with the reduced low dimensional feature vector. Such techniques are not well suited for large scale applications. In this work, we address this problem by reducing the search space. We investigate for a fast and accurate mechanism to index the face databases.

In this paper, we propose an indexing technique to narrow down the search space. First, we preprocess the face image to detect face part from the background and enhance the intensity values of the extracted face image. We detect Speed Up Robust Feature (SURF) key points [27, 35] in different scale spaces of the preprocessed face images and extract SURF feature descriptors at each key point. We generate a set of sixty eight dimensional index keys from the key points, feature descriptors and identity of a face image. Among these the first four dimensions of index keys are used to create a two-level index space. The first level index space divides all face images into two groups depending on the value of the first dimension. In the second level index space, we create two index cubes based on the other three dimensions. Each cell of an index cube keeps the reference of a kd-tree where we store the feature descriptors and the identity of a set of face images. We apply a set of hash functions on the index keys to find the cell positions for face images. At the time of identification, we apply the same hash functions on the query key points and search the kd-tree to retrieve a small set of similar identities from the index space. Finally, we rank all retrieved identities according to their occurrences.

The rest of the paper is organized as follows. In Section 2, we discuss the existing face indexing techniques for face biometric identification system. We briefly describe the preprocessing task in Section 3. In Section 4, we discuss our proposed approach for face indexing. The experimental results are presented in Section 5. Finally, the paper concludes in Section 6.

## 2. RELATED WORK

In the existing literature, very few work have been reported for face indexing to reduce the search space. We describe these techniques [28, 29, 30] in this section. Lin et al. [28] proposed an indexing structure to search the face from a large database. They compute a set of eigenfaces based on the faces in the database. Then, they assign a rank to each face in the database according to its projection onto each of the eigenface. Similarly, they compute the eigenfaces for a query and rank a query face. They select a set of faces from the database corresponding to the nearest faces in the ranked position with respect to each eigenface of the query face. These selected faces are used for recognition.

Mohanty et al. [29] propose a linear subspace approximation method for face indexing. They build a linear model to create a subspace-based on the match scores. They apply a linear transformation to project face images into the linear subspace. To do this, first, they apply a rigid transformation obtained through principal component analysis and then a non-rigid, affine transformation. They use an iterative stress minimization algorithm to obtain a distance matrix in a low-dimensional space and propose a linear out-of-sample projection scheme for test images. Any new face image is projected into this embedded space using an affine transformation.

Kaushik et al. [30] propose a modified geometric hashing technique to index the face database. They extract features from a face image using Speeded-Up Robust Features (SURF) operator.

They apply mean centering, principal component analysis, rotation and normalization to preprocess the SURF features. Finally, they use geometric hashing to hash these features to index each facial image in the database.

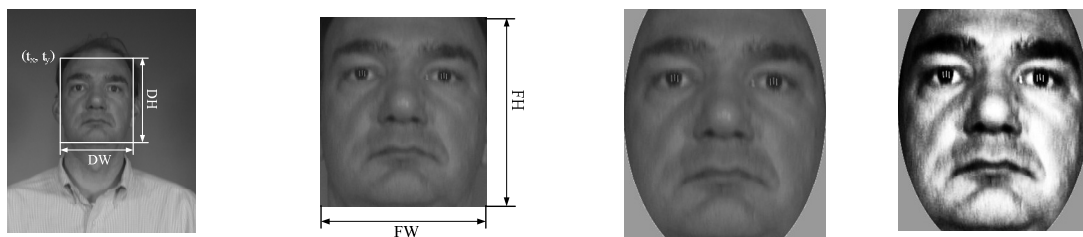
The major concern in eigenface and linear approximation method is the number of computations at the time of selecting top matches from the database. The number of computations in eigenface based method [28] depends on the number of eigenfaces considered for matching. To achieve good recognition rate a large number of eigenfaces are needed to consider and this does not give much computational advantages over the linear methods. The Linear subspace approximation method [29] does not give computational advantages when linear projection on raw templates (such as PCA, LDA etc.) are used for matching because the computation time for matching two face images in the database and mapping of face images into linear model space are same. The main concern in the geometric hashing technique is the selection of basis points for hashing [31, 32]. Wrong selection of basis points may deteriorate the performance of the geometric hashing based face indexing. Another problem in geometric hashing technique is that more number of basis points selection leads to the more computation time in indexing technique.

### 3. PREPROCESSING

Input face image of a biometric system contains background and is not necessarily good quality. To extract the features from a face image we need to enhance the image. This makes feature extraction task easy and ensures the quality of the extracted features. The steps followed in the preprocessing are briefly described in the following.

#### 3.1 Geometric Normalization

The input face images may not be in same size and align in the same direction (due to movement of head at the time of capturing). We follow geometric normalization process of Bolme et al. [33] and Beveridge et al. [53] to align and scale the images so that the face images are in the same position, same size and at same orientation. To get the geometric normalized image, first, we rotate the face image by an angle such that the eye coordinates are in same line with the horizontal axis. After rotating the face image, we detect the face part from the rotated image. To do this we use Viola & Jones [34] face detection algorithm. The detected face is shown in Fig. 1(a). To make the face image scale invariant, we map the detected face part ( $DW \times DH$ ) into a fixed size image ( $FW \times FH$ ) by applying scaling transformation. Figure 1(b) shows the fixed size image of width  $FW$  and height  $FH$ .



(a) Detected face boundary (b) Detected face image mapped into fixed size image (c) Masked face image (d) Enhanced face image after masking

**FIGURE 1:** Face Images after Different Preprocessing Tasks.

#### 3.2 Face Masking

We apply masking to separate the foreground region from the background region of a face image. The foreground region is corresponding to the clear face area which is the area of interest. This area contains the significant feature values. We mask the face image to ensure that the face recognition system does not respond to features corresponding to background, hair, clothing etc. We use an elliptical mask [33, 53] such that only the face from forehead to chin and left cheek to

right cheek is visible. Figure 1(c) shows the face image after applying the elliptical mask on the geometric normalized image where only face part is present in the image and background is masked out.

### 3.3 Intensity Enhancement

Intensity enhancement is required to reduce image variation due to lighting and sensor differences. We do the intensity enhancement in two steps [33]. First, we equalize the histogram of the unmasked face part and then normalize the intensity of the image to a mean of zero and standard deviation of one. Figure 1(d) shows the intensity enhancement image of the masked face image.

## 4. PROPOSED APPROACH

Speed-Up-Robust-Feature (SURF) [35, 27] method is known as a good image interest points (also called key points) and feature descriptors detector. We apply SURF method in our approach. We use SURF feature extraction method because it has several advantages over other feature extraction methods. The most important property of an interest point detector using SURF method is its repeatability. Repeatability means that the same interest points will be detected in different scales, orientations and illuminations of a given image. Another advantage is that the SURF method is computationally very fast. In addition to these, the SURF feature provides scale, rotation and illumination invariant feature descriptors.

Figure 2 shows the different tasks in enrollment and identification process of our approach. Both enrollment and identification processes have four common tasks as shown in Figure 2. In this section, first we present the key point extraction steps followed by orientation calculation of each key point. Then we discuss the feature descriptor extraction at each key point followed by the index key generation. Then, we describe index space creation and storing of index keys. Finally, we discuss the querying method to retrieve the identity from the index space.

### 4.1 Key Point Detection

We follow Bay et al. [27, 35] method to detect key points from an face image. The method consists of three steps.

In first step, we create scale spaces of the preprocessed image, which helps us to detect key points at different scales of the image. We construct eight distinct Gaussian filters with different sizes and different standard deviations. Then, we convolve the image with these Gaussian filters.

In next step, we calculate Hessian-matrix [27, 36] at each pixel position in the different scale space images. To compute the Hessian-matrix, we use integral images [27] to reduce the computation time of key point detection. We detect the key points based on the determinant values of the Hessian matrices. Note that all detected key points are not necessarily discriminant because the determinant of the Hessian Matrix does not produce local maximum or minimum

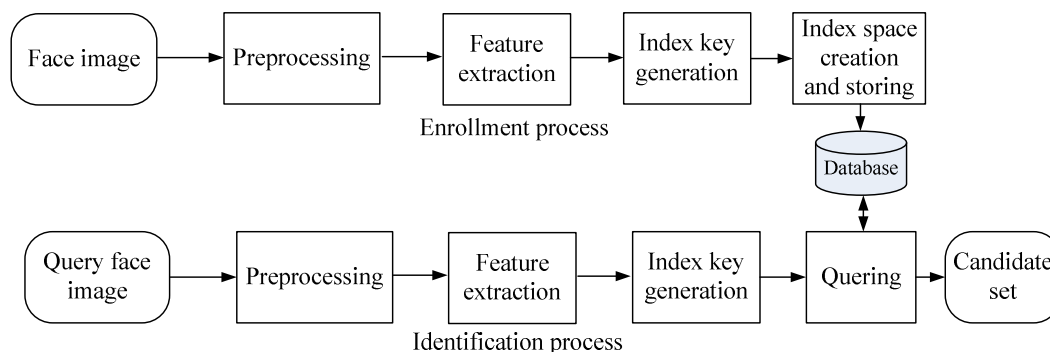


FIGURE 2: Overview of the Proposed Approach.

response at all detected points.

Finally, the most discriminant key points are localized from all the detected key points. To do this, first, we consider those points whose the determinant value is high and remove the points whose values are less than a threshold value. Bay et al. [35] shows that the threshold value 600 is good for detecting the discriminant key points from an image with average contrast and sharpness. Then, we perform non-maximal suppression to find the candidate key points. We do it by comparing each key point with its neighbors and finding the local maxima. We localize the key points by interpolating the maxima of the determinant of the Hessian matrix in scale and image spaces.

#### 4.2 Orientation Assignment

We assign an orientation to a key point to extract rotation invariant features from the face image. The orientation is important because we extract the feature descriptors relative to this orientation in later stage. We follow Bay et al. [27, 35] method to compute the orientation at each key point. To find the orientation of a key point, first, we create a circular area centered with the key point. Then, we calculate the Haar wavelet responses [37] at each key point within the circular area in  $x$  and  $y$  direction and compute the weighted responses of the Haar wavelet responses with a Gaussian filter. The weighted response is represented by a point in the vector space. We find the dominating orientation at each key point by calculating the resultant vector in a window of size 60 degree. The longest vector leads as orientation of the key point.

A set of key points is detected from an image and we estimate orientation of each key point. A key point can be represented with position, orientation, scale space in which the key point is detected, Laplacian value and the determinant of Hessian matrix. Let  $k_1, k_2, \dots, k_L$  be the  $L$  detected key points of an input image. We represent the key points of an image as shown in Eq. (1).

$$\begin{aligned}
 k_1 &= x_1 \ y_1 \ \theta_1 \ \sigma_1 \ l_{s_1} \ h_{s_1} \\
 k_2 &= x_2 \ y_2 \ \theta_2 \ \sigma_2 \ l_{s_2} \ h_{s_2} \\
 &\dots \ \dots \\
 k_L &= x_L \ y_L \ \theta_L \ \sigma_L \ l_{s_L} \ h_{s_L}
 \end{aligned} \tag{1}$$

In Eq. (1),  $(x, y)$  and  $\theta$  represent the position and orientation of a key point, respectively;  $\sigma_i$  ( $i=1,2, \dots, \delta$ ) denotes scale space at which key point is detected;  $l_s$  and  $h_s$  represent the Laplacian value and determinant of Hessian matrix, respectively.

#### 4.3 Key Point Descriptor Extraction

In this step, we extract the feature descriptors at each key point from the scale space images as follows. Scale space images are created by applying Gaussian filter on the images (as discussed in Section 4.1). We follow SURF method Bay et al. [27] to extract the feature descriptors from the face image. First, we create a square window of size  $20\sigma$  where  $\sigma$  is the scale or standard deviation of the Gaussian filter at which key point is detected. The window is centered at key point position and the direction of window is the same with the orientation of the key point (see Fig. 3). Now, the window is divided into  $4 \times 4$  square sub regions and within each sub-region  $25$  ( $5 \times 5$ ) regularly distributed sample points are placed. We calculate Haar wavelet responses [37] at each sample point of a sub-region in  $x$  and  $y$  directions. We weight the Haar wavelet responses with a Gaussian filter with standard deviation  $3.3\sigma$  centered at key point to reduce the effect of geometric deformations and localization errors. Let  $dx$  and  $dy$  be the Haar wavelet responses at each sample point within each sub-region. We consider  $\sum dx$ ,  $\sum |dx|$ ,  $\sum dy$  and  $\sum |dy|$  as four features at each sub-region. Hence, we create  $64$  ( $4 \times 4 \times 4$ ) descriptors corresponding to each key point. In Eq. (2),  $d_1, d_2, \dots, d_i, \dots, d_L$  represent descriptors of  $L$  key points and  $f_i^j$  represents the  $j^{\text{th}}$  descriptor of the  $i^{\text{th}}$  key point.

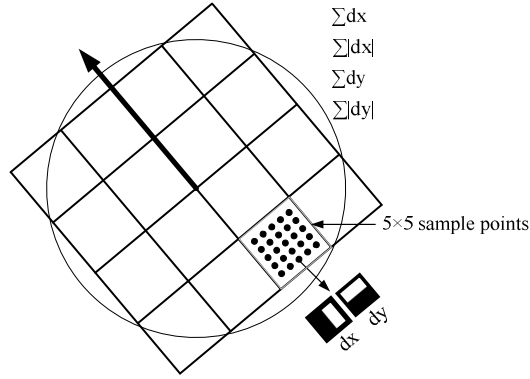


FIGURE 3: SURF Descriptor Extraction at a Key Point.

$$\begin{aligned}
 d_1 &= f_1^1 \ f_1^2 \ f_1^3 \ \dots \ f_1^j \ \dots \ f_1^{64} \\
 \dots & \dots \\
 d_i &= f_i^1 \ f_i^2 \ f_i^3 \ \dots \ f_i^j \ \dots \ f_i^{64} \\
 \dots & \dots \\
 d_L &= f_L^1 \ f_L^2 \ f_L^3 \ \dots \ f_L^j \ \dots \ f_L^{64}
 \end{aligned} \tag{2}$$

#### 4.4 Index Key Generation

We extract all key points and feature descriptors from all face images. We can represent a face image with a set of index keys. The set of index keys are generated from the extracted key points of a face image such that for each key point there is an index key. More precisely, we use key point information, feature descriptors and identity of person as the constituents of an index key. We represent an index key as a row vector of sixty nine elements. The first four values of an index key contain the sign of Laplacian, position and orientation of a key point. Next sixty four values of the index key hold the feature descriptors corresponding to the key point and the last value keeps the identity of a person. The first four values are used to index the database and the feature descriptors are used to search the identity of a person. Let  $L_p$  be the number of key points ( ${}^p k_1, \dots, {}^p k_{L_p}$ ) and feature descriptors ( ${}^p d_1, \dots, {}^p d_{L_p}$ ) extracted from the  $p^{th}$  face image. Note that  $L_p$  may vary from one face image to another. Thus,  $L_p$  number of index keys are generated for the  $p^{th}$  face image. We represent the index keys of the  $p^{th}$  person in Eq. (3). The  $i^{th}$  index key ( ${}^p indx_i$ ) of the  $p^{th}$  face image is generated by the  $i^{th}$  key point ( ${}^p k_i$ ) and corresponding feature descriptors ( ${}^p d_i$ ), and the identity ( $id^p$ ) of the  $p^{th}$  face image. In Eq. (3),  ${}^p ls_i, {}^p x_i, {}^p y_i, {}^p \theta_i$  and  ${}^p d_i$  represent the sign of Laplacian,  $x$  and  $y$  positions, orientation and feature descriptors of the  $i^{th}$  key point ( ${}^p k_i$ ), and  $id^p$  represents the identity of the  $p^{th}$  face image.

$$\begin{aligned}
 indx_1^p &= {}^p ls_1 \quad {}^p x_1 \quad {}^p y_1 \quad {}^p \theta_1 \quad {}^p d_1 \quad id^p \\
 indx_2^p &= {}^p ls_2 \quad {}^p x_2 \quad {}^p y_2 \quad {}^p \theta_2 \quad {}^p d_2 \quad id^p \\
 \dots & \dots \\
 indx_i^p &= {}^p ls_i \quad {}^p x_i \quad {}^p y_i \quad {}^p \theta_i \quad {}^p d_i \quad id^p \\
 \dots & \dots \\
 indx_{L_p}^p &= {}^p ls_{L_p} \quad {}^p x_{L_p} \quad {}^p y_{L_p} \quad {}^p \theta_{L_p} \quad {}^p d_{L_p} \quad id^p
 \end{aligned} \tag{3}$$

#### 4.5 Index Space Creation and Storing

Once the index keys are generated, we have to create an index space to store all index keys into the database. The created index space helps us to find a match corresponding to a query in fast and accurate manner. To create index space, we use first four components of an index key. These are the sign of Laplacian ( $ls$ ), positions ( $x$  and  $y$ ) and orientation  $\theta$  of a key point. All index keys can be classified into two groups based on the sign of the Laplacian value ( $ls$ ) because this value distinguishes the brightness (dark and light) at a key point position. Note that all face images are aligned in the same direction and scaled to the same size in the preprocessing step. Hence, a key point will occur at the same or near to the same position in the image and the orientation of the key point will remain almost same although, the face images are captured at different time. So, we can divide the index keys in each group into sub-groups based on the positions ( $x$  and  $y$ ) and orientation ( $\theta$ ) of a key point.

Due to the above characteristics of key points we propose a two-level index space to store the index keys. In the first level, we divide the index space based on the value of  $ls$  of index keys. The value of  $ls$  can be either '-1' for low intensity value or '+1' for high intensity value for a key point. Hence, the first level index space ( $LS$ ) is divided into two sub-index spaces ( $LS_0$  and  $LS_1$ ) as shown in Fig. 4. In the second level, each sub-index space is divided into a number of cells based on the positions ( $x$  and  $y$ ) and orientation ( $\theta$ ) of key points. We represent the second level index space ( $INDX$ ) as a three dimensional index space. The three dimensions of index space are  $x$ ,  $y$  and  $\theta$ . Each dimension is in different scales. To bring each dimension in same scale we normalize the each dimension. To do this we quantize each dimension of the second level index space into the same number of units. Each dimension is quantized into  $\delta$  number of units. The value of  $\delta$  is decided experimentally (discussed in Section 5). We refer each three dimensional index space in the second level as an index cube. Each index cube contains  $\delta^3$  number of cells. Figure 4 shows two three-dimension index cubes for storing the index keys.

Now, we store all index keys into the index space based on the first four values of the index keys. Note that a number of index keys may map into a single cell of an index cube because index values of a set of index keys may fall within the same range. We find the cell positions for all index keys. To do this we define a set of hash functions based on the sign value of Laplacian, positions and orientation of a key point. Let  $ls$ ,  $(x, y)$  and  $\theta$  be the sign value of Laplacian, positions and orientation of a key point, respectively. Then the hash functions are defined in Eq. (4). In Eq. (4),  $ls'$ ,  $x'$ ,  $y'$ , and  $\theta'$  are the cell index of the two-level index space and  $FH$  and  $FW$

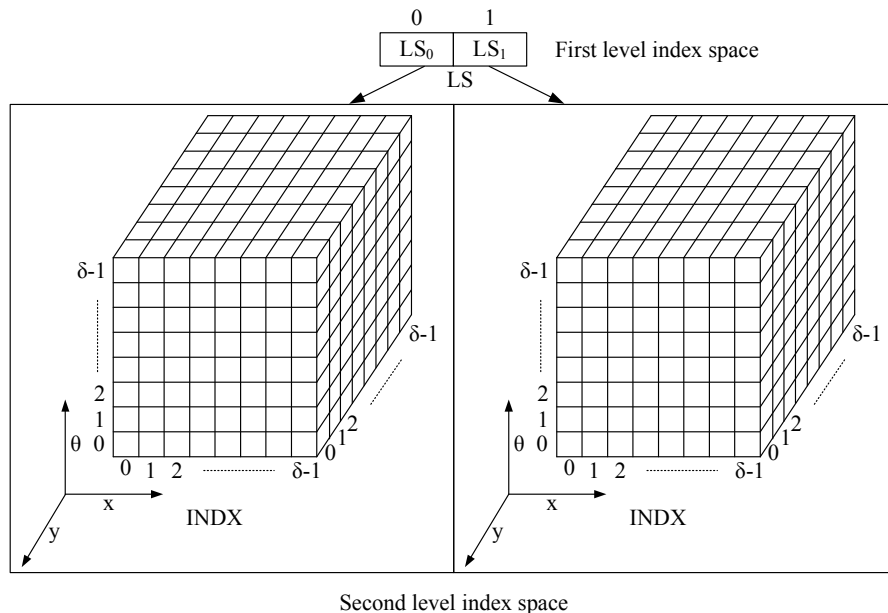


**FIGURE 4:** Proposed index space to store all index keys of all face images. represent the height and width of the normalized face image, respectively.

$$\begin{aligned}
 ls' &= H_{ls}(ls), \text{ where } H_{ls}(ls) = \frac{ls+1}{2} \\
 x' &= H_x(x), \text{ where } H_x(x) = \left\lfloor \frac{x \times \delta}{FW} \right\rfloor \\
 y' &= H_y(y), \text{ where } H_y(y) = \left\lfloor \frac{y \times \delta}{FH} \right\rfloor \\
 \theta' &= H_\theta(\theta), \text{ where } H_\theta(\theta) = \left\lfloor \frac{\theta \times \delta}{360} \right\rfloor
 \end{aligned} \tag{4}$$

We illustrate the storing of an index key into the proposed two-level index space with an example. Let  $indx = \langle ls = -1, x=55, y=89, \theta=45, d_1, d_2, \dots, d_{64}, id \rangle$  be an index key of a face image of size  $130 \times 150$  ( $FW \times FH$ ),  $d_1$  to  $d_{64}$  are the 64 dimensional feature descriptors of that key point and  $id$  be the identity of the subject. To store the feature descriptors ( $d_1, d_2, \dots, d_{64}$ ) and the identity ( $id$ ) into the index space, we apply the hash functions (defined in Eq. (4)) on  $ls, x, y$  and  $\theta$  of the key point. The feature descriptors will be stored into the first index cube ( $LS_0$ ) of the first level of index space because the value of  $ls'$  is 0 after applying the hash function on  $ls$ . The cell position of the index cube in second level index space ( $INDX$ ) is decided by applying the hash function on  $x, y$  and  $\theta$ . Let us assume that each dimension of second level index space is divided into 15 units (i.e.  $\delta = 15$ ). After applying the hash function on  $x, y$  and  $\theta$  the value of  $x', y'$  and  $\theta'$  are 6, 8 and 1, respectively. Hence, the feature descriptors ( $d_1, d_2, \dots, d_{64}$ ) and identity ( $id$ ) of the index key ( $indx$ ) is stored at  $[6,8,1]$  location in the first index cube which is represented as  $LS_0 \rightarrow INDX[6][8][1]$ .

We may note that a cell of an index cube can contain a set of index keys. To store the index keys we propose two storing structures: linear storing structure and kd-tree storing structure. These storing structures are discussed in the following.

#### 4.5.1 Linear Storing Structure

In this technique, we create a two-dimensional linear index space ( $LNINDEX$ ) for each cell of the index cube. Each linear index space is assigned a unique id ( $lid$ ) and this id is stored in the corresponding cell of the index cube. Note that there are  $\delta^3$  number of cells in each index cube. Hence,  $2\delta^3$  number of linear index spaces is created to store all index keys using linear storage structure. The linear index space ( $LNINDEX$ ) stores the 64-dimensional feature descriptors ( $d_1, d_2, \dots, d_{64}$ ) of index keys and identities ( $id$ ) of individuals. The size of the linear index space ( $LNINDEX$ ) is  $N \times (D+1)$  where  $N$  is the number of index keys in the cell and  $D$  is the number of feature descriptors within an index key. We store all index keys of a cell into the linear index space ( $LNINDEX$ ) for that cell. Figure 5 shows the linear index space for a cell of an index cube. In Fig. 5,  $LNINDEX_i$  is the linear index space for the  $i^{th}$  cell of the first index cube ( $LS[0] \rightarrow INDX$ ). The cell stores the id ( $lid$ ) of the linear index space ( $LNINDEX_i$ ). The  $i^{th}$  cell of the index cube  $LS[0] \rightarrow INDX$  is represented as  $CELL[i]$ . The method for creating linear index space is summarized in Algorithm 1. In Step 6 of Algorithm 1, we find the index cube from the first level index space. The cell position of the index cube is found in Step 7 to Step 9. Step 10 calculates the id of linear index space and Step 11 assigns that id to a cell of an index cube. We copy the descriptor values and the identities of index keys in Step 12 and 13.



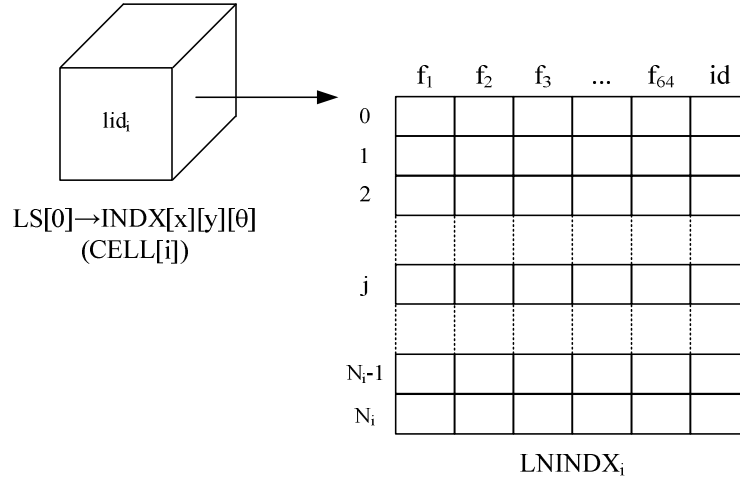


FIGURE 5: Linear indexing to store all index keys in  $i^{th}$  cell of the index space.

---

**Algorithm 1** Creating index space with linear storing structure

---

**Input:** All index keys of all person's face image ( $indx_1^p, indx_2^p, \dots, indx_{L_p}^p$ ; for  $p=1$  to  $P$ ). Two level index space ( $LS[] \rightarrow INDX[][][]$ ).

**Output:** Index space ( $LS[] \rightarrow INDX[][][]$ ) with linearly stored index keys for each cell ( $CELL[] \rightarrow LNINDEX[][]$ )

1. **for**  $c=0$  to  $2 \times \delta^3 - 1$  **do**
  2.      $inc[c] = 0$  //Initialize linear index counter
  3. **end for**
  4. **for**  $p=1$  to  $P$  **do**
  5.     **for**  $i=1$  to  $L_p$  **do**
  6.          $ls = H_{ls}(ls_i^p)$  //Decide first level index space  
        //Decide cell location of second level index space
  7.          $x = H_x(x_i^p)$
  8.          $y = H_y(y_i^p)$
  9.          $\theta = H_\theta(\theta_i^p)$
  10.          $lid = ls \times \delta^3 + x \times \delta^2 + y \times \delta + \theta$  //Calculate id for linear index space
  11.          $LS[ls] \rightarrow INDX[x][y][\theta] = lid$  //Copy id of linear index space into a cell
  12.          $CELL[lid] \rightarrow LNINDEX[inc[lid]] = {}^p d_i$  //Copy descriptor values of index key into linear index space
  13.          $CELL[lid] \rightarrow LNINDEX[inc[lid]][65] = id^p$  //Copy identity of person into linear index space
  14.          $inc[lid] = inc[lid] + 1$  //Increment linear index counter
  15.     **end for**
  16. **end for**
- 

**4.5.2 Kd-tree Storing Structure**

In this technique, we create a kd-tree for each cell of an index cube and assign a unique identity ( $kid$ ) to the each kd-tree. The identity of the kd-tree is stored into the corresponding cell of the index cube. There are  $2\delta^3$  number of cells in the index space. Hence, the total number of kd-trees

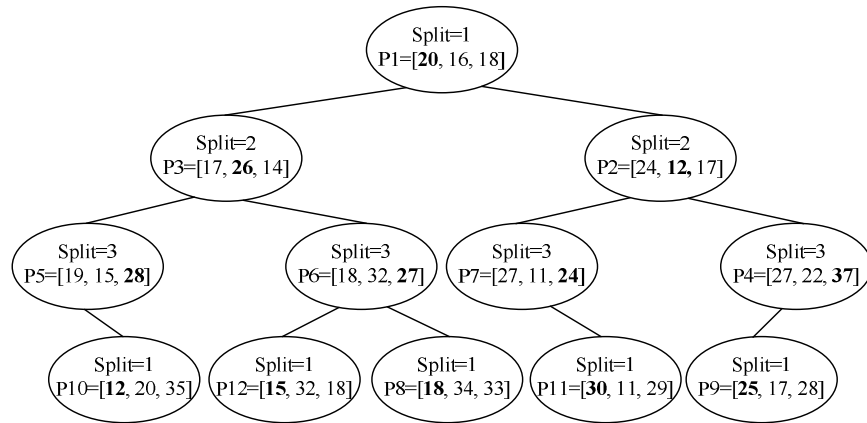
required is  $2\delta^3$ . All index keys of a cell are stored into a kd-tree. A kd-tree is a data structure for storing a finite set of points from a k-dimensional space [38]. The kd-tree is a binary tree in which every node stores a k-dimensional point. In other words, the node of a kd-tree stores an eight dimensional point. The node structure of kd-tree is shown in Fig. 6(a). In a node of kd-tree, *keyVector* field stores the k-dimensional index key and *Split* field stores the splitting dimension or a discriminator value. *leftTree* and *rightTree* store a kd-tree representing the pointers to the left and the right of the splitting plane, respectively. For an example, let there are eleven number of three dimensional points ( $P_1, P_2, \dots, P_{11}$ ) as shown in Fig. 6(b) and *kd-tree* with these points is shown in Fig. 6(c). We insert the first point  $P_1$  at the root of the *kd-tree*. At the time of insertion, we choose one of the dimensions as a basis (*Split*) of dividing the rest of the points. In this example, the value of *Split* in the root node is 1. In other words, if the value of the first dimension of the current point to be inserted is less than the same of the root, then the point is stored in *leftTree* otherwise in *rightTree*. This means all items to the left of root will have the first dimension value less than that of the root and all items to the right of the root will have greater than (or equal to) that of the root. The point  $P_2$  is inserted in the right kd-tree and  $P_3$  is inserted in the left *kd-tree* of the root. When we insert the point  $P_4$ , we first compare the first dimension value of  $P_4$  with the root and then compare the second dimension value of  $P_4$  with the second dimension value of  $P_2$  at next level. The point  $P_4$  is inserted in the right *kd-tree* of the point  $P_2$ . Similarly, we insert all other points into the kd-tree. First dimension will be chosen again as the basis (*Split*=1) for discrimination at level 3.

keyVector: k-dimensional point
Split: splitting dimension
leftTree: A kd-tree representing the points to the left of the splitting plane
rightTree: A kd-tree representing the points to the right of the splitting plane

- |                 |                  |
|-----------------|------------------|
| P1 = <20 16 18> | P7 = <27 11 24>  |
| P2 = <24 12 17> | P8 = <18 34 33>  |
| P3 = <17 26 14> | P9 = <25 17 28>  |
| P4 = <27 22 37> | P10 = <12 20 35> |
| P5 = <19 15 28> | P11 = <30 11 29> |
| P6 = <18 32 27> | P12 = <15 32 18> |

(a) Components of a kd-tree node

(b) Sample 3D points



(c) Kd-tree example

**FIGURE 6:** Structure of a kd-tree and an example of kd-tree with 3-dimensional points.

We store all sixty four dimensional points (descriptors of an index key) within a cell in a kd-tree data structure. To store the index keys we apply the method proposed by Arya and Mount [54, 55] which follows Bentley [38] kd-tree insertion method. The maximum height of the optimized kd-tree with N number of k-dimensional point is  $\lceil \log_2(N) \rceil$  [40]. The kd-tree structure for the  $i^{th}$  cell is shown in Fig. 7. In Fig. 7,  $KDINDX_i$  is the kd-tree for the  $i^{th}$  cell of the first index cube ( $LS[0] \rightarrow INDX$ ). The cell stores the identity (*kid*) of the kd-tree ( $KDINDX_i$ ). The  $i^{th}$  cell of the first index cube  $LS[0] \rightarrow INDX$  is represented as  $CELL[i]$ . We summarize the method for creating kd-



8.  $y = H_y(y_i^p)$
9.  $\theta = H_\theta(\theta_i^p)$
10.  $kid = ls \times \delta^3 + x \times \delta^2 + y \times \delta + \theta$  //Calculate id for kd-tree index space
11.  $LS[ls] \rightarrow INDX[x][y][\theta] = kid$  //Copy id of the kd-tree into a cell
12.  $Temp[] = {}^p d_i$  //Copy descriptors of index key into temporary vector
13.  $Temp[65] = id^p$  //Copy identity of person into the temporary vector
14. Insert  $Temp$  into  $Kd-tree_{kid}$
15.  $inc[kid] = inc[kid] + 1$  //Increment kd-tree index counter
16. **end for**
17. **end for**

The  $i^{th}$  query index key is represented as  $indx_i^q = {}^q ls_i, {}^q x_i, {}^q y_i, {}^q \theta_i, {}^q d_i, id^q$  where  ${}^q ls_i, {}^q x_i, {}^q y_i$  and  ${}^q \theta_i$  represent the sign of Laplacian,  $x$  and  $y$  position, and orientation of the  $i^{th}$  key point ( ${}^q k_i$ ), and  ${}^q d_i$  and  $id^q$  represent the feature descriptor of the  $i^{th}$  key point and identity of the query face image, respectively. Then, we apply indexing on the first level index space using the value of  $ls$  of the query index key. The indexing is done using hash functions defined in Eq. (4). The first level of indexing selects the index cube for a query index key. Let us assume that the value of  $ls$  of the  $i^{th}$  index key of query is -1. Then index cube ( $LS[0] \rightarrow INDX$ ) in the first level index space ( $LS$ ) is selected for the  $i^{th}$  index key of the query. Then, we use the value of  $x, y$  and  $\theta$  of the query index key to find the cell position of the index cube in the second level index space. The cell position is calculated using the hash functions defined in Eq. (4). Then, the candidate set is generated by counting the vote received for each identity of the retrieved index keys from the database. A candidate set  $CS$  is shown in Fig. 8. The  $id$  and  $vote$  fields of the  $CS$  store the identity of an individual and the number of vote received for that identity. The candidate set is generated for every type of searching. To generate the candidate set we search the corresponding linear or kd-tree storage whose identity is stored in the cell of an index cube and find the closest match in the linear or kd-tree index space. If  $x, y$  and  $\theta$  of the  $i^{th}$  index key of a query select the  $LS[0] \rightarrow INDX[x][y][\theta]$  cell of the index cube ( $LS[0] \rightarrow INDX$ ) and retrieve the  $i^{th}$  linear or kd-tree identity then we find the closest match in the  $LNINDEX_i$  linear index space for linear search and  $KDTREE_i$  for kd-tree search. Finally, ranks are calculated based on the vote received for each identity. The search techniques are described in the following.

#### 4.6.1 Linear Search

In linear search, first we find the cell position in an index cube for a query index key. Then, we search the linear index space of that cell. We compute Euclidean distance between feature descriptor of a query index key and all the feature descriptors stored in the linear index space to find a match. Let the  $j^{th}$  cell in the index cube is selected for the  $i^{th}$  index key of a query. Then, we select the linear index space ( $CELL[j] \rightarrow LNINDEX$ ) corresponding to the  $j^{th}$  cell to find a match. We compute the Euclidean distances between the feature descriptors of the  $i^{th}$  index key of the query and all the descriptors stored in the linear index space ( $CELL[j] \rightarrow LNINDEX$ ) using Eq. (6). We retrieve the identity corresponding to the minimum distance. The retrieved identity is then placed in the candidate set ( $CS$ ) and cast a vote for this identity. We follow the same procedure for all other index keys of the query face. We summarize the linear searching method in Algorithm 3. In Step 2 of Algorithm 3, we initialize the length of each linear index space. Step 6 and Steps 7 to 9 find the index of the first and second level index spaces, respectively. We calculate the cell id in Step 10. In Steps 11 to 19, we find the minimum distance for an index key of query face and retrieve the identity corresponding to the minimum distance. Steps 23 to 29 generate the candidate set for a query index key. Finally, we sort the candidate set in Step 33.

$$ED_{i,j} = EuclidDist(d_j, {}^q d_i),$$

$$\text{where, } EuclidDist(d_j, {}^q d_i) = \sum_{f=1}^{64} (d_j^f - {}^q d_i^f)^2 \quad (6)$$

#### 4.6.2 Kd-tree Search

In kd-tree search, first we find the cell position in an index cube for an index key of a query. Then we retrieve the id of a kd-tree (*kid*) from the cell and search the kd-tree corresponding to the retrieved kd-tree id. We apply hash functions to find the cell position in the index cube. Let the  $j^{th}$  cell in the index cube is selected for the  $i^{th}$  query index key. Then we search kd-tree index space ( $CELL[j] \rightarrow KDINDEX$ ) corresponding to the  $j^{th}$  cell to find a match. We apply approximate nearest neighbor search [54, 55, 56, 57] to reduce the searching time. Arya and Mount's [54, 56] approximate k nearest neighbor search method is used to search the kd-tree. In this technique, we examine only the k closest bins of the kd-tree and use a priority queue to identify the closest bins based their distances from query. The expected searching complexity of the nearest neighbor search can be reduced to  $O(kd \log n)$  and space complexity is  $O(dn)$ . For this purpose, a public domain library (FLANN) [56, 57] for faster approximate nearest neighbors search is available. In our approach, we utilize this library for implementing kd-tree algorithms. We retrieve the identity corresponding to the closest match from the kd-tree. The retrieved identity is then placed in the candidate set (*CS*) and cast a vote for this identity. We follow the same procedure for all other index keys of the query face. The searching method for kd-tree index space is summarized in Algorithm 4. Step 3 and Steps 4 to 6 of Algorithm 4 find the index of the first and second level index spaces, respectively. In Step 7, we calculate the cell id of an index cube for a query index key. Step 8 finds the nearest neighbor for a query index key and Step 9 retrieves the identity corresponding to the nearest neighbor. In Steps 11 to 15, we generate the candidate set for a query index key. Finally, we sort the candidate set in Step 18.

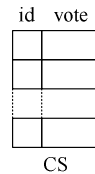


FIGURE 8: Schematic view of the candidate set.

---

#### Algorithm 3 Candidate set generation in linear search from index space

---

**Input:** All index keys from query face image  $indx_1^q, indx_2^p, \dots, indx_{L_q}^q$ , index space ( $LS[] \rightarrow INDX[][][]$ ) with linearly stored index keys for each cell ( $CELL[] \rightarrow LNINDEX[][]$ ).

**Output:** Candidate Set ( $CS[] \rightarrow (id, vote)$ )

1. **for**  $cellid = 0$  to  $2 \times \delta^3 - 1$  **do** //Initialize length in each linear index space
2.      $KEYS[cellid] =$  Number of keys in  $CELL[cellid] \rightarrow LNINDEX[][]$
3. **end for**
4.  $idc = 1$
5. **for**  $i = 1$  to  $L_q$  **do** // $L_q$  is the total number of query index key
6.      $ls' = H_{ls}(ls_i^q)$  //Find first level index space  
      //Find cell location of second level index space
7.      $x' = H_x(x_i^q)$
8.      $y' = H_y(y_i^q)$
9.      $\theta' = H_\theta(\theta_i^q)$
10.     $cellid = LS[ls'] \rightarrow INDX[x'][y'][\theta']$  //Calculate cell id of an index cube  
      //Retrieve the matched identities from  $CELL[cellid] \rightarrow LNINDEX[][]$
11.     $MinDist = \infty$
12.    **for**  $j = 0$  to  $KEYS[cellid] - 1$  **do** // $KEYS[cellid]$  is the total number of index key in the  $cellid^{th}$  cell
13.        $ED_{i,j} = EucladDist(CELL[cellid] \rightarrow LNINDEX[j], qd_i)$

```

14.   if  $ED_{ij} \leq MinDist$  then //Find match identities corresponding to the minimum distance
15.        $m = 1$ 
16.        $MatchId[m] = CELL[cellid] \rightarrow LNINDEX[j][65]$ 
17.   else if  $ED_{ij} = MinDist$  then
18.        $m = m + 1$ 
19.        $MatchId[m] = CELL[cellid] \rightarrow LNINDEX[j][65]$ 
20.   end if
21. end for
22. for  $j = 1$  to  $m$  do
23.      $id = MatchId[m]$ 
24.     if  $id \notin CS[ ] \rightarrow (id)$  then //Generate candidate set
25.        $CS[idc] \rightarrow id = id$ 
26.        $CS[idc] \rightarrow vote = 1$ 
27.        $idc = idc + 1$ 
28.     else
29.        $CS[id] \rightarrow vote = CS[id] \rightarrow vote + 1$ 
30.     end if
31.   end for
32. end for
33. Sort  $CS[ ] \rightarrow (id, vote)$  in descending order based on  $vote$ 

```

---

**Algorithm 4** Candidate set generation in kd-tree search from index space

**Input:** All index keys from query face image  $indx_1^q, indx_2^p, \dots, indx_{L_q}^q$ , index space ( $LS[ ] \rightarrow INDX[ ][ ][ ]$ ) with kd-tree index space for each cell ( $CELL[ ] \rightarrow KDINDEX[ ]$ ).

**Output:** Candidate Set ( $CS[ ] \rightarrow (id, vote)$ )

```

1.   $idc = 1$ 
2.  for  $i = 1$  to  $L_q$  do //  $L_q$  is the total number of query index key
3.     $ls' = H_{ls}(ls_i^q)$  //Find first level index space
    //Find cell location of second level index space
4.     $x' = H_x(x_i^q)$ 
5.     $y' = H_y(y_i^q)$ 
6.     $\theta' = H_\theta(\theta_i^q)$ 
7.     $cellid = LS[ls] \rightarrow INDX[x'][y'][\theta']$  //Calculate cell id of an index cube
    //Retrieve the matched identities from Kd-tree ( $Kd-tree_{cellid}$ ) by finding nearest
    neighbor of a query index key
8.     $NN = findNN(Kd-tree_{cellid},^q d_i)$  //Find the nearest neighbor
9.     $id = retrieveIdFromNN(NN)$  //Select id of nearest neighbor
10.  if  $id \notin CS[ ] \rightarrow (id)$  then //Generate candidate set
11.     $CS[idc] \rightarrow id = id$ 
12.     $CS[idc] \rightarrow vote = 1$ 
13.     $idc = idc + 1$ 
14.  else
15.     $CS[id] \rightarrow vote = CS[id] \rightarrow vote + 1$ 
16.  end if
17. end for
18. Sort  $CS[ ] \rightarrow (id, vote)$  in descending order based on  $vote$ 

```

---

#### 4.7 Analysis of the Proposed Approach

In this section, we analyze the time complexity of linear and kd-tree based search techniques in the proposed index space. We also analyze the memory requirement of the proposed method.

##### 4.7.1 Searching Time Complexity

Let  $N$  be the total number of face images enrolled in the database and  $T_p$  be the average number of index keys in each enrolled face image. Thus, the total number of index keys in the index space is  $T_n = T_p \times N$ . If there are  $K$  number of cells in all index cubes, then the average number of index keys in each cell is  $T_k = T_n/K$ . Let  $T_q$  be the average number of index keys in each query face image. To perform linear search or kd-tree based search in the index space, first, we find the index cell position for a index key of a query using hash functions defined in Eq.(4). This operation requires  $O(1)$  computation time for both type of searches. The time complexity analysis of linear and kd-tree based searches within the located cell are given in the following.

**Linear Search:** In linear search,  $T_k \times T_q$  number of comparisons are required to retrieve a set of similar index keys and their identities, and  $T_q \log T_q$  comparisons are required to sort the retrieved identities based on their ranks. Thus, we can calculate the average time complexity of linear search (denoted as  $T_{LS}$ ) as follows.

$$\begin{aligned} T_{LS} &= O(1) \times T_q + T_k \times T_q + T_q \log T_q \\ &= O(1) \times T_q + \frac{N \times T_p}{K} \times T_q + T_q \log T_q \\ &= O(N) \end{aligned} \tag{7}$$

**Kd-tree Search:** The number of comparisons required in kd-tree based search to find a set of nearest index keys and their identities are  $\log T_k \times T_q$ , and to sort the retrieved identities based on their ranks are  $T_q \log T_q$ . Thus, we can calculate the average time complexity of kd-tree based search (denoted as  $T_{KS}$ ) as follows.

$$\begin{aligned} T_{KS} &= O(1) \times T_q + \log T_k \times T_q + T_q \log T_q \\ &= O(1) \times T_q + \log \frac{N \times T_p}{K} \times T_q + T_q \log T_q \\ &= O(\log N) \end{aligned} \tag{8}$$

##### 4.7.2 Memory Requirement

Let  $b_1$  and  $b_2$  bytes memory are required to store the reference of the index cubes into the first level index space and the reference of linear or kd-tree index spaces into the index cube, respectively. Let  $m$  bytes are required to store a feature value of an index key and 2 bytes are required to store an identity of an individual. If there are  $P$  individuals then we can compute the memory requirement for linear and kd-tree index spaces using Eq. (9) and (10), respectively. In Eq. (9) and (10),  $L_p$  represents the number of index keys for the  $p^{th}$  individual and  $\delta$  denotes the number of quantization levels of the second level index space.

$$M_{LS} = 2 \times (b_1 + \delta^3 \times b_2) + \sum_{p=1}^P (64 \times m + 2) \times L_p \tag{9}$$

$$M_{KD} = 2 \times (b_1 + \delta^3 \times b_2) + \sum_{p=1}^P (64 \times m + 14) \times L_p \tag{10}$$

## 5. EXPERIMENTS AND EXPERIMENTAL RESULTS

This section describes the different experimental setups and the experimental results to evaluate the accuracy and the efficiency of our proposed approach.

## 5.1 Database

We perform our experiments on two widely used large face databases namely Color FERET [40, 41, 42] and FRGC V2.0 [43, 44, 45]. We also carry out our experiments on CalTech 256 [46, 47] face database. A detail description of each database is given in the following.

### 5.1.1 Color FERET Face Database

The FERET database is developed for the Facial Recognition Technology (FERET) program [41, 42]. The database is designed by the Defense Advanced Research Products Agency (DARPA) during 1993 to 1997 to give common standard for face recognition experiments. The database contains 11338 images from 994 different subjects. These images are collected in different sessions. The resolution of the captured images is 256×384 pixel. The database contains 2722 frontal images with different facial expressions (Neutral and Alternate). There are 1364 images with neutral expression and 1358 images with alternate expression. Figure 9(a) and (b) shows the four images with different facial expressions of two different subjects.

### 5.1.2 FRGC 2.0 Face Database

FRGC Still version 2.0 data set [43, 44, 45] is collected at University of Notre Dame as a part of Face Recognition Grand Challenge program. The primary goal of the FRGC program is to promote and advance the face recognition technology designed to support existing face recognition systems. This database contains color face images, which are taken in different lightning conditions and different environments. The database consists of 24038 frontal face images of 466 subjects. These images are captured in Fall 2003 and Spring 2004 semesters of 2003-2004 academic year. A total of 16024 images from all subjects are captured in indoor environment with two different protocols (FERET and Mugshot) and two different facial expressions (Neutral and Smiley) [43]. The resolution of each image is either 1704×2272 pixel or 1200×1600 pixel. The images are collected in 4007 subject sessions. Four images (FERET-Neutral, FERET-Smiley, Mugshot-Neutral and Mugshot-Smiley) are captured in each subject session. The database contains 4007 FERET-Neutral, 4007 FERET-Smiley, 4007 Mugshot-Neutral and 4007 Mugshot-Smiley face images. Figure 9(c) and (d) show four images with two facial expressions of two different subjects. FRGC Still version 2.0 data set [43, 44, 45] contains 8014 face images which are captured in outdoor environment with different backgrounds and different illuminations. Figure 9(e) shows two face images of two different subjects in different backgrounds.

### 5.1.3 CalTech 256 Face Database

Caltech-256 object category data set [47, 46] contains a total of 30607 images from 256 different categories. In our experiment, we use face category images of the Caltech-256 data set. The face category set consists of 432 face images from 28 subjects. Each face image is captured in complex background with different facial expressions. Figure 9(f) shows two face images of two different subjects from CalTech 256 face database.

## 5.2 Implementation Environment

All methods described in our approach are implemented using C programming language and OpenCV [48] image processing library on the Linux operating system. All methods are evaluated with Intel Core-2 Duo processor of speed 2.00GHz and 2GB RAM.



### 5.3 Performance Metrics

Accuracy and efficiency are the two main criteria usually considered to measure the performance of a face indexing technique. The accuracy of a face indexing approach is commonly evaluated

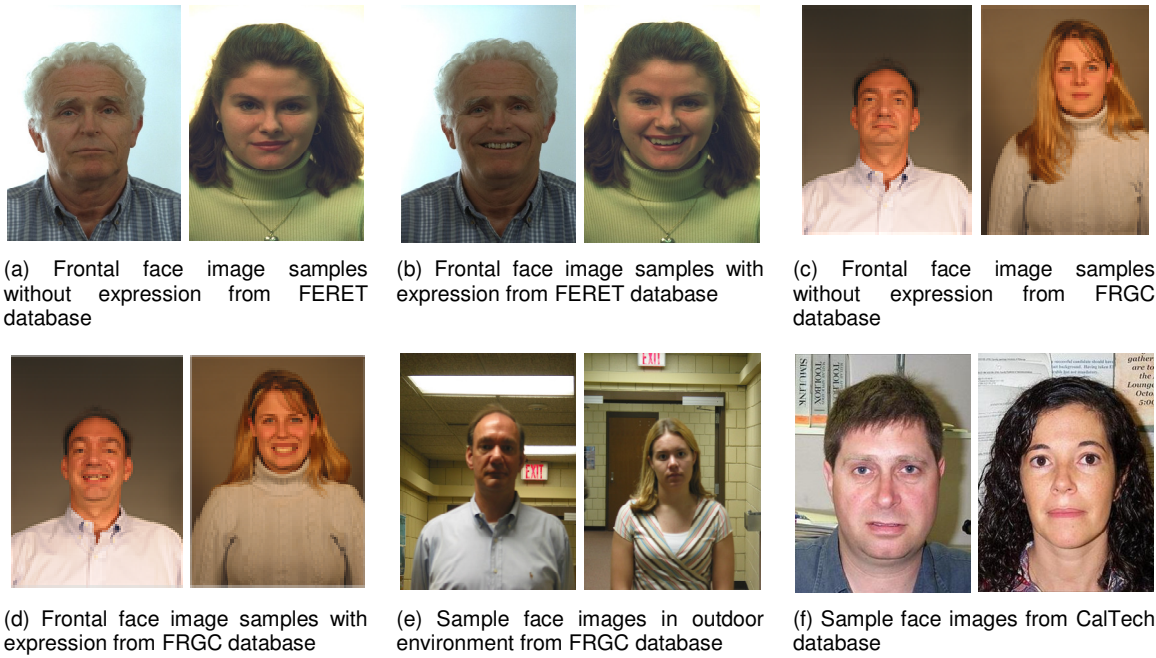


**FIGURE 9:** Sample images of FERET, FRGC and CalTech256 databases.

by the hit rate or recognition rate, and penetration rate [49, 50, 51, 52]. Hit rate is the percentage of probes for which the correct identities are retrieved within a top rank for a gallery by the indexing mechanism [50]. The penetration rate is the percentage of the database retrieved for a query face to get a correct match [50]. Let  $N_g$  be the number of entries in the database and  $N_p$  be the number of queries in the probe set. If  $N_r$  is the number of entries retrieved for the  $i^{th}$  probe then the penetration rate ( $PR$ ) for a query is defined as in Eq. (11). If  $N_c$  ( $N_c < N_p$ ) is the number of queries for which successful matches are found within the top  $r$  retrieved candidates then the hit rate ( $HR$ ) at rank  $r$  is defined as Eq. (12)

$$PR = \frac{1}{N_p} \sum_{i=1}^{N_p} \frac{N_r}{N_g} \quad (11)$$

$$HR = \frac{N_c}{N_p} \quad (12)$$

We also substantiate our results in terms of cumulative match score. The cumulative match score gives the probability of at least one correct identity presents within a top rank which also represents the cumulative hit rate at different ranks. The cumulative hit rates at different ranks are represented with the Cumulative Match Characteristics (CMC) curve.

### 5.4 Evaluation Setup

To evaluate our proposed indexing method, we have partitioned each face database into two sets: *Gallery Set* and *Probe Set*. *Gallery Set* contains the face images which are enrolled into the index database and *Probe Set* contains the face images which are used as queries to search the index database. In our experiment, we create different gallery and probe sets for each database.

The description of different gallery and probe sets for FERET, FRGC and CalTech256 databases are given in Table 1.

### 5.5 Experiments and Results

We have conducted a number of experiments to evaluate the performance of our proposed indexing methods. The description of these experiments and the results of each experiment are given in the following.

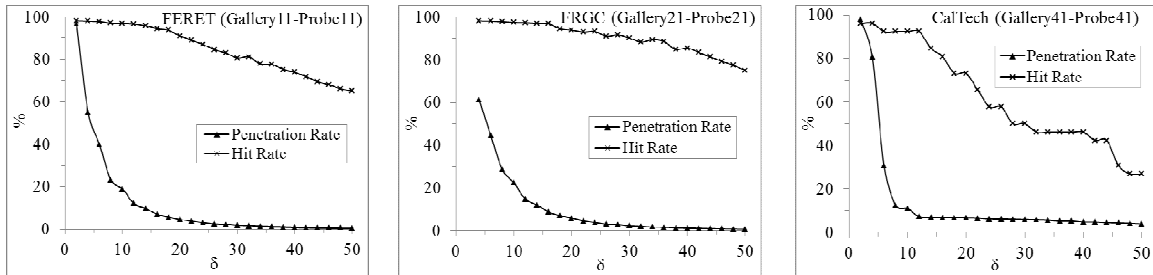
#### 5.5.1 Experiment 1: Determining dimension quantization value of second level index space

To determine the value of the number of quantization ( $\delta$ ) of each dimension of the second level index space, we have done this experiment. We perform kd-tree based search for a set of query images with different values of  $\delta$ . The value of  $\delta$  is varied from 2 to 50 with increment of 2. This experiment is conducted with FERET, FRGC and CalTech databases. We use *Gallery11* and *Probe11* for FERET database, *Gallery21* and *Probe21* for FRGC database, and *Gallery41* and *Probe41* for CalTech database. The rank 1 hit rate and penetration rate for different values of  $\delta$  are reported in Fig. 10. From Fig. 10(a), we observe that for FERET database rank 1 hit rate decreases nearly 2% when the value of  $\delta$  is changed 2 to 14 whereas rank 1 hit rate decreases more than 4% when the value of  $\delta$  is changed 16 to 20. On the other hand, the penetration rate decreases more than 85% when the value of  $\delta$  is changed 2 to 14 but penetration rate decreases only 5% for the change of  $\delta$  value 14 to 20 for FERET database. The same thing is observed from Fig. 10(b) for FRGC database also. But for Caltech database the value of  $\delta$  equal to 12 gives better performance than the other values of  $\delta$  (see Fig. 10(c)). Hence, in our other experiments, we choose the value of  $\delta$  equal to 15 for FERET and FRGC databases, and 12 for Caltech database, respectively. However, user may choose the other values of  $\delta$  according to their requirements.

DB	Name	# images	# subjects	Description
Color FERET	Gallery11	994	994	First face image with neutral facial expression of first session for all subjects.
	Gallery12	1984	992	First face image with neutral and alternate facial expressions of first session for all subjects.
	Probe11	992	992	First face image with alternate facial expression of first session for all subjects.
	Probe12	370	250	Face images with neutral facial expressions of other sessions for all subjects.
	Probe13	366	247	Face images with alternate facial expressions of other sessions for all subjects.
	Probe14	736	250	Face images with neutral and alternate facial expressions of other sessions for all subjects.
FRGC V2.0	Probe15	228	75	Face images with neutral and alternate facial expressions of other sessions for all subjects. But images are captured with minimum six months difference.
	Gallery21	466	466	First face image with neutral facial expression of first session for all subjects. Images are captured with FERET protocol.
	Gallery22	932	466	First face image with neutral and smiley facial expressions of first session for all subjects. Images are captured with FERET protocol.
	Probe21	466	466	First face image with smiley facial expression of first session for all subjects. Images are captured with FERET protocol.
	Probe22	3541	411	Face images with neutral facial expressions of other sessions for all subjects. Images are captured with FERET protocol
	Probe23	3541	411	Face images with smiley facial expressions of other sessions for all subjects. Images are captured with FERET protocol.
	Probe24	7082	411	Face images with neutral and smiley facial expressions of other sessions for all subjects. Images are captured with FERET protocol
Probe25	1134	193	Face images with neutral and smiley facial expressions of other sessions for all subjects. Images are captured with FERET protocol. The time difference from first	

			captured image is minimum six months.	
Probe26	466	466	First face image with neutral facial expression of first session for all subjects. Images are captured with Mugshot protocol.	
Probe27	466	466	First face image with smiley facial expression of first session for all subjects. Images are captured with Mugshot protocol.	
Probe28	3541	411	Face images with neutral facial expressions of other sessions for all subjects. Images are captured with Mugshot protocol	
Probe29	3541	411	Face images with smiley facial expressions of other sessions for all subjects. Images are captured with Mugshot protocol.	
Probe30	7082	411	Face images with neutral and smiley facial expressions of other sessions for all subjects. Images are captured with Mugshot protocol	
Probe31	1134	193	Face images with neutral and smiley facial expressions of other sessions for all subjects. Images are captured with Mugshot protocol. The time difference from first captured image is minimum six months.	
Probe32	8014	466	Face images with at outdoor environment.	
CalTech256	Gallery41	28	28	One face image from each subject. Face image is selected randomly.
	Gallery42	28	350	Eighty percent face images of each subject. Face images are selected randomly.
	Probe41	26	26	One face image from each subject. Face image is selected randomly from the rest of the Gallery1.
	Probe42	26	404	All face images of each subject except the Gallery 1 face images.
	Probe43	26	82	All face images of each subject except the Gallery 2 face images.

TABLE 1: Description of gallery and probe sets of FERET, FRGC and CalTech256 face databases.



(a) Hit rate and penetration rate with FERET Gallery11 and Probe11 sets for different values of  $\delta$

(b) Hit rate and penetration rate with FRGC Gallery21 and Probe21 sets for different values of  $\delta$

(c) Hit rate and penetration rate with CalTech256 Gallery41 and Probe41 sets for different values of  $\delta$

FIGURE 10: HR and PR with FERET, FRGC and CalTech256 databases for different values of  $\delta$

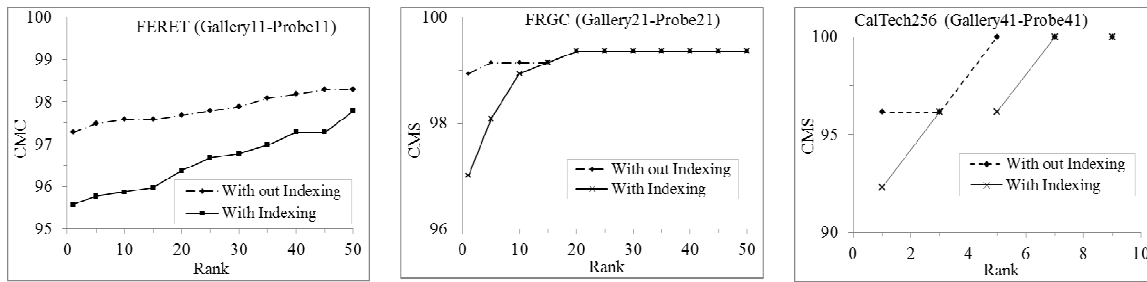
5.5.2 Experiment 2: Performance comparison without and with indexing

In this experiment, we compare the performance of the system with and without applying the proposed indexing technique. We use *Gallery11* and *Probe11* for FERET, *Gallery21* and *Probe21* for FRGC databases, and *Gallery41* and *Probe41* for CalTech databases. The CMC curves with and without indexing for different databases are shown in Fig. 11. Figure 11(a) shows that the approach without indexing gives better cumulative match score for FERET database. Whereas, From Fig. 11(b) and (c), we can see that the approach with and without indexing gives almost the same cumulative match score after 15<sup>th</sup> rank for FRGC database and after 7<sup>th</sup> rank for the CalTech database. We also report the rank 1 hit rate, penetration rate and average searching time for linear and kd-tree search using indexing and without indexing in Table 2. From Table 2, we can see that kd-tree search with indexing achieves 95.57%, 97% and 92.31% hit rate with 9.70%, 12.55% and 7.14% penetration rate for FERET, FRGC and CalTech databases,

Database	Performance	Linear		Kd-tree	
		Without Indexing	With Indexing	Without Indexing	With Indexing
FERET	Hit Rate	97.28	95.57	97.28	95.57
	Penetration Rate	100	10.54	49.43	7.90
	Average Search Time	$4.46 \times 10^5$	114	$2.21 \times 10^5$	85.40
FRGC	Hit Rate	98.93	97.00	98.93	97.00
	Penetration Rate	100	16.36	51.47	12.55
	Average Search Time	$2.78 \times 10^5$	92.55	$1.43 \times 10^5$	71.02
CalTech	Hit Rate	96.15	92.31	96.15	92.31
	Penetration Rate	100	26.91	61.78	23.72
	Average Search Time	$1.24 \times 10^4$	8.10	$7.64 \times 10^3$	7.14

**TABLE 2:** Comparison of the proposed approach with and without indexing using linear and kd-tree search.

respectively. We also observe that kd-tree search requires very less average searching time for all three databases.



(a) CMC curve with and without indexing for FERET Gallery11 and Probe11 sets

(b) CMC curve with and without indexing for FRGC Gallery21 and Probe21 sets

(c) CMC curve with and without indexing for CalTech256 Gallery41 and Probe41 sets

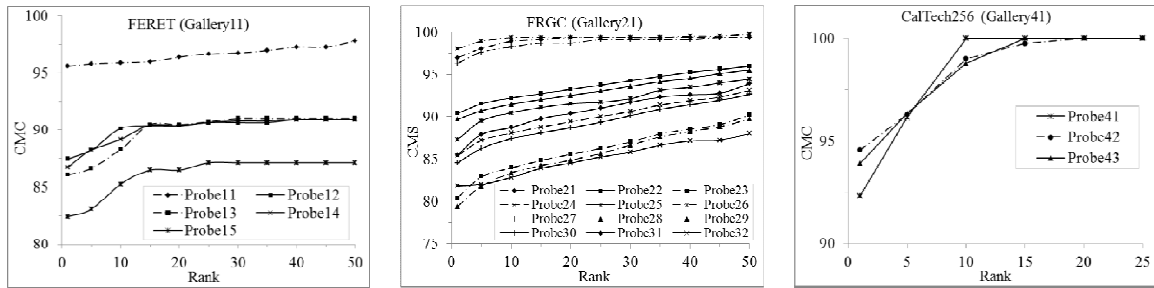
**FIGURE 11:** CMC curve with and without indexing for FERET, FRGC and CalTech256 databases.

### 5.5.3 Experiment 3: Performance with different probe sets

In this experiment, we check the performance of linear and kd-tree search with the proposed indexing method for different probe sets. The probe sets are created with different conditions as discussed in Table 1. We enroll the all images of *Gallery11* (with neutral expression), *Gallery21* (with neutral expression) and *Gallery41* into the database for FERET, FRGC and CalTech databases, respectively and use all probe sets to test the indexing performances of linear and kd-tree search. Figure 12(a) shows the CMC curve of all five probe sets of FERET database, Fig. 12(b) shows the CMC curve of all twelve probe sets of FRGC database and Fig. 12(c) shows the CMC curve of all three probe sets of CalTech database. From Fig. 12(a) and (b), we can note that cumulative match scores are reduced for the probe sets which contain the face images captured in more than six month difference. On the other hand, face images captured in different expressions but in the same session give the better results than the others. We observe that face images with complex background (*Probe32* of FRGC database) gives less match score than the others. However, face images with complex background for CalTech database give above 90% match score. We also report the rank 1 hit rate, penetration rate and searching time for linear and kd-tree search for different probe sets in Table 3. We observe that the penetration rate and searching time for kd-tree based search are less for all probe sets.

**5.5.4 Experiment 4: Performance of multiple enrolments of a subject into the index space**

We have done the experiment to check the effect of multiple enrolments on the performance. In this experiment, we enroll all samples of *Gallery12* for FERET, *Gallery22* for FRGC and *Gallery42* for CalTech databases, and test with all probe sets of FERET, FRGC and CalTech databases. The CMC curves of all probe sets are shown in Fig. 13. From Fig. 13, we can see that 100% cumulative match score is achieved for *Probe11* and *Probe21* because the images in the *Probe11* and *Probe21* sets are also in the *Gallery12* and *Gallery22*, respectively. We observe that in multiple enrolments of a subject, cumulative match scores for other probe sets are increased than that of in the single enrolments. We have computed the penetration rate, rank 1 hit rate and searching time for linear and kd-tree based search with multiple enrolments. The results are summarized in Table 4. From this experiment we observe that better rank 1 hit rate is achieved without affecting the penetration rate. Though, higher searching time is required to search the database with multiple enrolments.



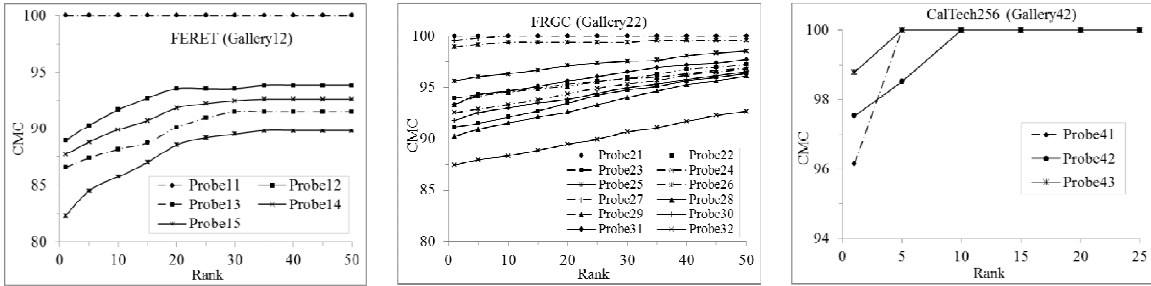
(a) CMC curves for different probe sets with FERET Gallery11 (b) CMC curves for different probe sets with FRGC Gallery21 (c) CMC curves for different probe sets with CalTech256 Gallery41

**FIGURE 12:** CMC curves for different probe sets with single enrolment of a subject with FERET, FRGC and CalTech256 databases

DB	Probe	Linear			Kd-tree		
		Hit rate	Penetration rate	Searching time (ms)	Hit rate	Penetration rate	Searching time (ms)
FERET	Probe11	95.57	10.54	114.00	95.57	7.90	85.40
	Probe12	87.44	11.13	121.98	87.44	8.34	91.38
	Probe13	86.11	11.28	122.32	86.11	8.45	91.64
	Probe14	86.75	11.20	121.29	86.75	8.39	90.87
	Probe15	82.44	10.62	114.29	82.44	7.96	85.62
FRGC	Probe21	97.00	16.36	92.55	97.00	12.55	71.02
	Probe22	90.40	14.66	82.48	90.40	11.25	63.29
	Probe23	80.41	16.13	92.01	80.41	12.38	70.60
	Probe24	85.40	15.40	87.66	85.40	11.81	67.27
	Probe25	87.31	15.69	88.48	87.31	12.04	67.89
	Probe26	98.07	14.62	81.73	98.07	11.22	62.71
	Probe27	96.36	16.20	91.73	96.36	12.43	70.39
	Probe28	89.70	14.41	81.72	89.70	11.06	62.71
	Probe29	79.39	16.07	91.24	79.39	12.33	70.01
	Probe30	84.54	15.24	84.86	84.54	11.69	65.12
	Probe31	85.46	15.42	86.88	85.46	11.83	66.67
	Probe32	81.40	15.47	86.38	81.81	11.87	66.28

CalTech	Probe41	92.31	26.91	8.19	92.31	23.72	7.22
	Probe42	94.55	27.52	8.29	94.55	24.27	7.31
	Probe43	93.90	27.72	8.48	93.90	24.44	7.47

TABLE 3: Performance of different probe sets with single enrolment of a subject in linear and kd-tree search.



(a) CMC curves for different probe sets with FERET Gallery12

(b) CMC curves for different probe sets with FRGC Gallery22

(c) CMC curves for different probe sets with CalTech256 Gallery42

FIGURE 13: CMC curves for different probe sets with multiple enrolment of a subject with FERET, FRGC and CalTech256 databases.

5.5.5 Experiment 5: False Match Rate (FMR) vs False Non Match Rate (FNMR)

We have analyzed the performance of our proposed system with respect to *false match rate (FMR)* and *false non match rate (FNMR)*. We use *Gallery11*, *Gallery21* and *Gallery42* datasets as gallery sets, and *Probe11*, *Probe21* and *Probe43* as probe sets for FERET, FRGC and CalTech databases, respectively. We have computed 992, 466 and 1297 genuine scores and 985056, 216690 and 27403 imposter scores for FERET, FRGC and CalTech databases, respectively. The receiver operating characteristics (ROC) curves show the trade-off between *FMR* and *FNMR* in Fig. 14. The equal error rates (ERR) of the system are 5.51%, 5.73% and 6.84% for FERET, FRGC and CalTech databases, respectively.

DB	Probe	Linear			Kd-tree		
		Hit rate	Penetration rate	Searching time(ms)	Hit rate	Penetration rate	Searching time(ms)
FERET	Probe11	100	9.33	207.66	100	6.74	149.98
	Probe12	88.94	9.85	215.93	88.94	7.11	155.96
	Probe13	86.56	9.99	216.59	86.56	7.21	156.43
	Probe14	87.73	9.92	214.91	87.73	7.16	155.22
	Probe15	82.31	9.40	205.35	82.31	6.79	148.31
FRGC	Probe21	100	13.69	164.07	100	10.14	121.54
	Probe22	91.11	12.27	146.87	91.11	9.09	108.79
	Probe23	93.93	13.50	163.63	93.93	10.00	121.21
	Probe24	92.52	12.88	153.78	92.52	9.54	113.91
	Probe25	95.59	13.13	157.14	95.59	9.73	116.40
	Probe26	98.93	12.23	148.34	98.93	9.06	109.88
	Probe27	99.57	13.56	160.79	99.57	10.04	119.11
	Probe28	90.23	12.06	144.72	90.23	8.93	107.20
	Probe29	93.31	13.45	160.29	93.31	9.96	118.73
Probe30	91.77	12.75	151.78	91.77	9.45	112.43	

	Probe31	93.30	12.90	151.07	93.30	9.56	111.90
	Probe32	87.00	12.94	153.26	87.44	9.59	113.53
CalTech	Probe41	96.15	14.21	55.70	96.15	11.12	43.58
	Probe42	97.52	14.54	57.35	97.52	11.38	44.87
	Probe43	98.78	14.64	57.85	98.78	11.46	45.27

**TABLE 4:** Performance of different probe sets for multiple enrolments of a subject in linear and kd-tree search.

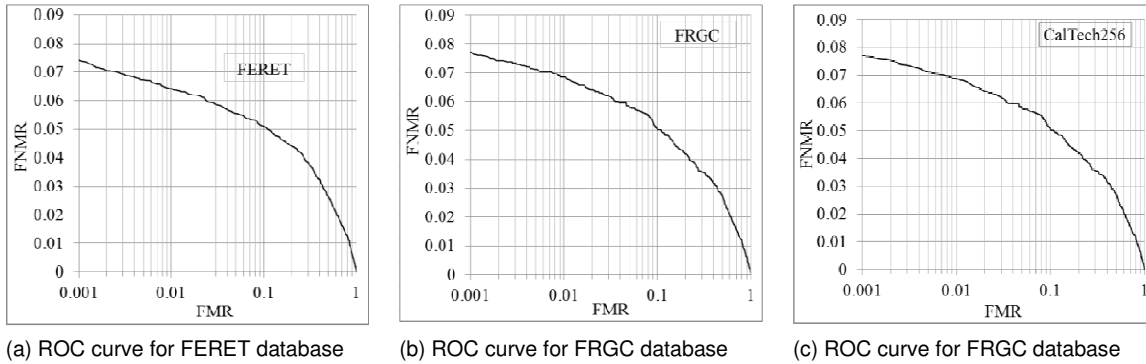


**FIGURE 14:** ROC curve for FERET, FRGC and CalTech256 databases.

**5.5.6 Experiment 6: Searching time with different number of enrolled samples**

In this section, we compute the searching time and the average number of comparisons required for linear and kd-tree based search techniques with the proposed index space. To compute these we enrolled different number of samples into the index space for FERET, FRGC and CalTech databases.

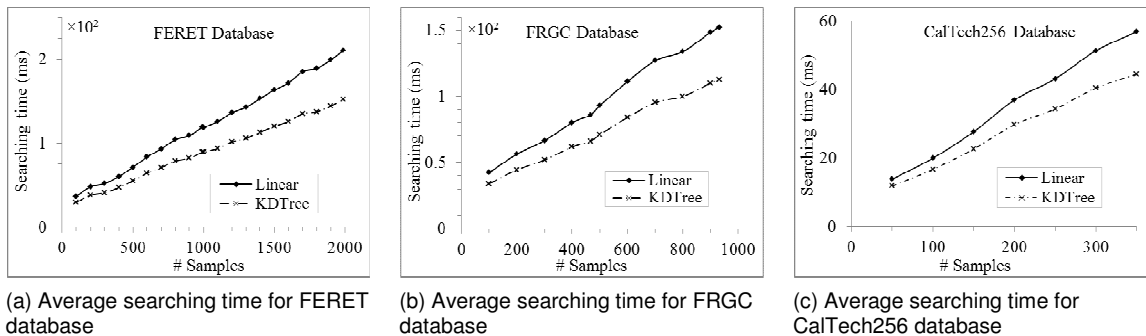
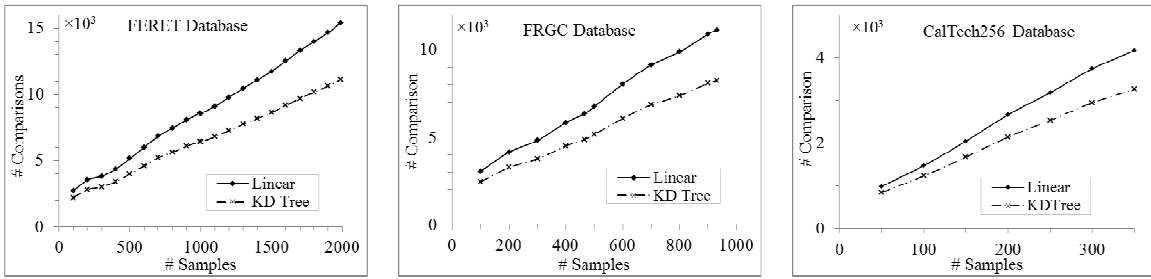


**FIGURE 15:** Average searching time with different sizes of databases for FERET, FRGC and CalTech256 databases.

The execution time (in Intel Core-2 Duo 2.00 GHz processor and 2GB RAM implementation environment) of linear and kd-tree search with FERET, FRGC and CalTech databases are shown in Fig. 15(a), (b) and (c), respectively. We observe that the execution time for kd-tree search is less than the linear search method. It is also observed that the rate of increment in execution time for kd-tree based search is less when the number of enrolled sample increases. We have given the average number of comparisons for linear and kd-tree based search in Fig. 16. From Fig. 16, we can see that the rate of increment in number comparisons is also less for kd-tree based search. Hence, we may conclude that to retrieve the similar identities for a given query, kd-tree based search within index cell is better than the linear search.

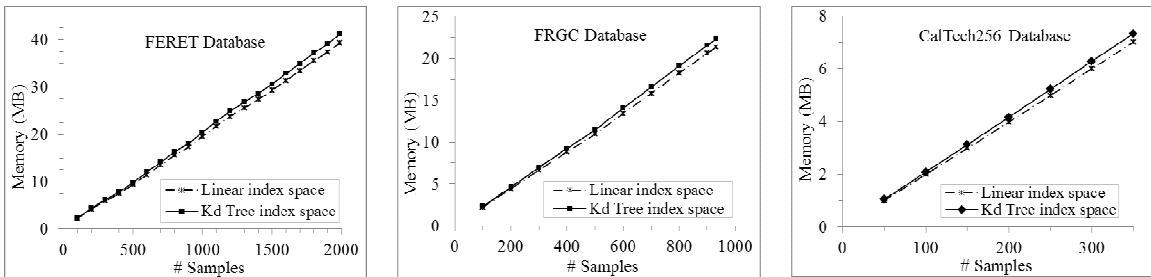


(a) Average number of comparisons for FERET database (b) Average number of comparisons for FRGC database (c) Average number of comparisons for CalTech256 database

**FIGURE 16:** Average number of comparisons with different sizes of databases for FERET, FRGC and CalTech256 databases.

**5.5.7 Experiment 7: Memory for different number of enrolled samples**

In our approach, 2 bytes are required to store the reference of index cube into a cell of first level index space and 4 bytes are required to store the reference of linear or kd-tree index space into a cell of index cube. There are 64 feature values in an index key and 4 bytes are required to store a feature value. We also store the identity of an individual with each index key. The identity field requires 2 bytes extra memory for each index key. We can store 216 identities with 2 byte identity field. Hence, a total of 258 bytes are required to store an index key along with the identity in linear index space. In kd-tree based index space, a single node of kd-tree requires 270 bytes memory. Fig. 17(a), (b) and (c) show the memory requirements for linear and kd-tree index spaces to store different number of samples for FERET, FRGC and CalTech databases, respectively. From Fig. 17 we observe that the memory requirements are almost same for the linear and kd-tree based index spaces.



(a) Memory requirements for FERET database (b) Memory requirements for FRGC database (c) Memory requirements for CalTech256 database

**FIGURE 17:** Memory requirements with different sizes of databases for FERET, FRGC and CalTech256 databases.

**5.6 Discussion of Experimental Results**

We have performed seven set of experiments to establish the accuracy and the efficiency of our proposed method. The first experiment is carried out to decide the parameter (number of the cells in an index cube). From this experiment, we observed that better penetration rate can be achieved by increasing the number of cells in index cube as it distributes the index key among more number of cells and it retrieved less number of keys at the time of querying. However, the probability of retrieving correct keys corresponding to the query is also reduced and it affects the hit rate of the identification system.

In experiment 2, we achieved less penetration rate when we apply indexing before identification. If we perform identification without indexing, query index keys are compared with the all stored



keys and the probability of matching is high at that time and we can achieve better hit rate but at the same time it increases the penetration rate. At the time of identification with indexing, probability of matching is reduced but the number of comparisons is also decreased which is reflected in the result of the second experiment.

There is an impact of sessions of capturing face images in the hit rate. From the third experiment, we can see that the performance of an indexing system is improved when we used the probe sets which are captured with less time gap. Further, the face image captured in indoor environment offers better performance. Further, if we consider the higher rank, the probability of matches will increase. The CMC curve shows the same trend of the hit rate in this experiment.

If we enroll multiple samples of a subject, the probability of matching a query subject will increase. From the fourth experiment, we observed that we achieved the maximum accuracy when we enrolled two samples per subject. It may be noted that accuracy of the system is improved if we enroll the samples with the different poses of a subject. Further, in the fifth experiment, we achieved better FMR and FNMR for the same reason.

As the searching complexity of the kd-tree is less than the linear search, we required less searching time when we used kd-tree in our indexing approach. The result of the sixth experiment substantiates that fact. If the number of samples for enrollment increases the memory requirement will also increase which we have shown in the seventh experiment.

### 5.7 Comparison with Existing Work

Lin et al. [28] propose an indexing structure to search the face from a large database. They compute a set of Eigenfaces based on the faces in the database. Then, they assign a rank to each face in the database according to its projection onto each of the Eigenface. Similarly, they compute the Eigenfaces for a query and rank a query face. Finally, they select a set of faces from the database corresponding to the nearest faces in the ranked position with respect to each Eigenface of the query face. These selected faces are used for recognition.

A linear subspace approximation method for face indexing has been developed by Mohanty et al. [29]. They build a linear model to create a subspace-based on the match scores. A linear transformation is applied to project face images into the linear subspace. For this purpose, first, they apply a rigid transformation obtained through principal component analysis and then a non-rigid affine transformation. An iterative stress minimization algorithm is used to obtain a distance matrix in a low-dimensional space and propose a linear out-of-sample projection scheme for test images. Any new face image is projected into this embedded space using an affine transformation.

Kaushik et al. [30] introduce a modified geometric hashing technique to index the face database. They extract features from a face image using SURF [27] operator. They apply mean centering, principal component analysis, rotation and normalization to preprocess the SURF features. Finally, they use geometric hashing to hash these features to index each facial image in the database.

We compare our approach with three existing face indexing approaches [28, 29, 30]. To compare our proposed work, we use *Gallery11*, *Gallery21* and *Gallery41* as gallery sets, and *Probe11*, *Probe21* and *Probe41* as probe sets for FERET, FRGC and CalTech databases, respectively. The comparison result is reported in Table 5. The comparison is done with respect to rank 1 hit rate, penetration rate and searching time. From Table 5 we can see that our approach gives better performance than existing approaches.

Approach	Performance	FERET	FRGC	CalTech
Lin et al. [28]	Hit Rate	83.87	85.19	73.08
	Penetration Rate	41.07	45.49	83.99
	Avg. Searching Time (ms)	2697.40	1738.35	895.27
Mohanty et al. [29]	Hit Rate	94.15	95.06	80.77
	Penetration Rate	25.58	24.95	60.5
	Avg. Searching Time (ms)	745.61	623.56	46.77
Kaushtik et al. [30]	Hit Rate	95.87	97.64	88.46
	Penetration Rate	16.96	18.61	27.49
	Avg. Searching Time (ms)	456.24	398.78	14.59
Proposed	Hit Rate	95.57	97.00	92.31
	Penetration Rate	7.90	12.55	23.72
	Avg. Searching Time (ms)	85.40	71.02	7.22

**TABLE 5:** Comparison of the proposed approach with existing approaches.

## 6. CONCLUSION AND FUTURE WORK

Face-based biometric identification system with a large pool of database requires huge computation time to search an individual's identity from the database. Best of our knowledge there is no good indexing technique exist for face identification system, which can identify a person in real-time when identification system is enrolled with a large number of users. In this work, we propose a new two-level indexing mechanism to reduce the search space for a face biometric-based identification system. We calculate a set of seventy dimensional index keys using SURF feature extraction method from a face image. Among seventy dimensions we consider only four dimensions to create the two-level index space. In the first level indexing, we group the index keys based on the sign of Laplacian value; and in the second level, we group the index keys based on the position and the orientation. We retrieve a set of similar identities for a query from the two-level index space using a hashing technique. The hashing technique requires  $O(1)$  time complexity to retrieve the identities. We propose linear and kd-tree based searching mechanism to search the identities within the two-level index space. We have tested our approach with FERET, FRGC and CalTech face databases. The experimental result shows that kd-tree based search is performed better than the linear search. We can achieve 95.57%, 97% and 92.31% rank 1 hit rate with 7.90%, 12.55% and 23.72% penetration rate for FERET, FRGC and CalTech databases, respectively. Our approach gives better hit rate when multiple samples of a subject are enrolled into the database. We achieve on the average 8.21%, 11.87% and 24.17% search space reduction for different probe sets of FERET, FRGC and CalTech, respectively. With our proposed indexing approach, we achieve the computation time advantage without compromising the accuracy compared to traditional person identification systems.

The limitation of our approach is that it does not give good results under different poses (e.g. left or right profile) of face images. Our work can be extended to address the limitation said above. Further, in this work, we have targeted the face images captured in the indoor environment. This work can be utilized for the face images captured in outdoor environment.

## 7. REFERENCES

- [1] T. Huang, Z. Xiong and Z. Zhang. Handbook of Face Recognition. NY: Springer, 2011, pp. 617–638.
- [2] H. Lee, S.-H. Lee, T. Kim and H. Bahn. “Secure User Identification for Consumer Electronics Devices.” IEEE Trans. on Consumer Electronics, vol. 54, no. 4, pp. 1798–1802, 2008.
- [3] D.-S. Kim, S.-Y. Lee, B.-S. Kim, S.-C. Lee and D.-H. Chung. “On the Design of an Embedded Biometric Smart Card Reader.” IEEE Trans. on Consumer Electronics. vol. 54, no. 2, pp. 573–577, 2008.
- [4] “Physical access control biometrics.” Internet: <http://www.findbiometrics.com/physical-access/> [Jun. 12, 2012].
- [5] “Biometrics from Wikipedia.” Internet: [http://en.wikipedia.org/wiki/Biometrics#Countries\\_applying\\_biometrics](http://en.wikipedia.org/wiki/Biometrics#Countries_applying_biometrics) [Jul. 15, 2012].
- [6] W. Louis and K. N. Plataniotis. “Frontal Face Detection for Surveillance Purposes using Dual Local Binary Patterns Features,” in Proc. 17th IEEE International Conference on Image Processing (ICIP), Sept 2010, pp. 3809–3812.
- [7] P. Quintiliano and A. Rosa. “Face Recognition Applied to Computer Forensics.” The International Journal of Forensic Computer Science, vol. 1, no. 1, pp. 19–27, 2006.
- [8] A. K. Jain, B. Klare and U. Park. “Face Matching and Retrieval in Forensics Applications.” IEEE Multimedia, vol. 19, no. 1, pp. 20–28, 2012.
- [9] “Using the Iris Recognition Immigration System (IRIS).” Internet: <http://www.ukba.homeoffice.gov.uk/customs-travel/Enteringtheuk/usingiris/> [Jan. 20, 2012].
- [10] “Biometric Passport from Wikipedia.” Internet: [http://en.wikipedia.org/wiki/Biometric\\_passport](http://en.wikipedia.org/wiki/Biometric_passport) [Jun. 22, 2012].
- [11] “Unique Identification Authority of India.” Internet: <http://uidai.gov.in/> [Jul. 12, 2012].
- [12] “Identity Document from Wikipedia.” Internet: [http://en.wikipedia.org/wiki/Identity\\_document#Bangladesh](http://en.wikipedia.org/wiki/Identity_document#Bangladesh) [Jul. 17, 2012].
- [13] Identity Card Policy, “List of National Identity Card Policies by Country.” Internet: [http://en.wikipedia.org/wiki/List\\_of\\_identity\\_card\\_policies\\_by\\_country](http://en.wikipedia.org/wiki/List_of_identity_card_policies_by_country) [Jun. 25, 2012].
- [14] “UIDAI Strategy Overview: Creating a Unique Identity Number for Every Resident in India.” Internet: [http://uidai.gov.in/UID\\_PDF/Front\\_Page\\_Articles/Documents/Strategy\\_Overveiw-001.pdf](http://uidai.gov.in/UID_PDF/Front_Page_Articles/Documents/Strategy_Overveiw-001.pdf) [May 18, 2012].
- [15] A. Mhatre, S. Palla, S. Chikkerur and V. Govindaraju. “Efficient Search and Retrieval in Biometric Databases.” in Proc. SPIE Defense and Security Symposium, vol. 5779, Orlando FL, Mar. 2005, pp. 265–273.
- [16] M. Turk and A. Pentland. “Eigenfaces for Recognition.” Journal of Cognitive Neuroscence, vol. 3, no. 1, pp. 71–86, 1991.
- [17] A. Batur and M. Hayes. “Linear Subspace for Illumination Robust Face Recognition.” in Proc. IEEE International Conference on Computer Vision and Pattern Recognition, Dec 2001.
- [18] P. Yuen and J. Lai. “Face Representation Using Independent Component Analysis.” Pattern Recognition, vol. 35, no. 6, pp. 1247–1257, 2002.
- [19] P. Belhumeur, J. Hespanha and D. Kriegman. “Eigenfaces vs. Fisherfaces: Recognition Using Class Specific Linear Projection.” IEEE Trans. on Pattern Analysis and Machine Intelligence, vol. 19, no. 7, pp. 711–720, 1997.

- [20] J. Lu, K. Plataniotis and A. Venetsanopoulos. "Face Recognition Using LDA-Based Algorithms." *IEEE Trans. on Neural Networks*, vol. 14, no. 1, pp. 195–200, 2003.
- [21] N. Mittal and E. Walia. "Face Recognition Using Improved Fast PCA Algorithm." in *Proc. Congress on Image and Signal Processing*, Sanya, Hainan, 2008, pp. 554–558.
- [22] S. T. Roweis and L. K. Saul. "Nonlinear Dimensionality Reduction by Locally Linear Embedding." *Science*, vol. 290, no. 5500, pp. 2323–2326, 2000.
- [23] T. Shakhunaga and K. Shigenari. "Decomposed Eigenface for Face Recognition under Various Lighting Conditions." in *Proc. IEEE International Conference on Computer Vision and Pattern Recognition*, Dec 2001.
- [24] W. Zhao, R. Chellappa, A. Rosenfeld and P. Phillips. "Face Recognition: A Literature Survey." *ACM Computing Surveys*, vol. 35, no. 4, pp. 399–458, 2003.
- [25] W. Yu, X. Teng and C. Liu. "Face Recognition Using Discriminant Locality Preserving Projections." *Image and Vision Computing*, vol. 24, no. 3, pp. 239–248, 2006.
- [26] X. He and P. Niyogi. "Locality Preserving Projections." in *Proc. Conference Advances In Neural Information Processing Systems 16*, 2003, pp. 153–160.
- [27] H. Bay, A. Ess, T. Tuytelaars and L. V. Gool. "SURF: Speeded Up Robust Features." *Computer Vision and Image Understanding*, vol. 110, no. 3, pp. 346–359, 2008.
- [28] K. H. Lin, K. M. Lam, X. Xie and W. C. Siu. "An Efficient Human Face Indexing Scheme Using Eigenfaces." in *Proc. IEEE International Conference on Neural Networks and Signal Processing*, 2003, pp. 920–923.
- [29] P. Mohanty, S. Sarkar, R. Kasturi and P. J. Phillips. "Subspace Approximation of Face Recognition Algorithms: An Empirical Study." *IEEE Trans. on Information Forensics and Security*, vol. 3, no. 4, pp. 734–748, 2008.
- [30] V. D. Kaushik, A. K. Gupta, U. Jayaraman and P. Gupta. "Modified Geometric Hashing for Face Database Indexing." in *Proc. 7th international conference on Advanced Intelligent Computing Theories and Applications: with Aspects of Artificial Intelligence*, 2011, pp. 608–613.
- [31] H. Wolfson and I. Rigoutsos. "Geometric Hashing: An Overview." *IEEE Computational Science and Engineering*, vol. 4, no. 4, pp. 10–21, 1997.
- [32] Y. Lamdan and H. J. Wolfson. "Geometric Hashing: A General and Efficient Model-based Recognition Scheme." in *Proceedings of the 2nd International Conference on Computer Vision*, 1988, pp. 238–249.
- [33] D. S. Bolme, J. R. Beveridge, M. L. Teixeira and B. Draper. "The CSU Face Identification Evaluation System: Its Purpose, Features and Structure." in *Proc. 3rd International Conf. on Computer Vision Systems*, 2003.
- [34] P. Viola and M. J. Jones. "Robust Real-time Face Detection." *International Journal of Computer Vision*, vol. 57, no. 2, pp. 137–154, 2004.
- [35] H. Bay, T. Tuytelaars and L. V. Gool. "SURF: Speeded Up Robust Features." in *Proc. 9th European Conference on Computer Vision*, vol. 3951, 2006, pp. 404–417.
- [36] T. Lindeberg. "Feature Detection with Automatic Scale Selection." *International Journal of Computer Vision*, vol. 30, no. 2, pp. 79–116, 1998.
- [37] A. Jensen and A. L. Cour-Harbo. *Ripples in Mathematics: The Discrete Wavelet Transform*. Springer, 2001.

- [38] J. L. Bentley. "Multidimensional Binary Search Trees Used for Associative Searching." *Communications of the ACM*, vol. 18, no. 9, pp. 509–517, 1975.
- [39] A. Moore. "A Tutorial on Kd-trees." Tech. Rep., University of Cambridge, 1991, Internet: <http://www.cs.cmu.edu/simawm/papers.html> [Nov. 20, 2011].
- [40] P. J. Phillips, H. Moon, S. A. Rizvi and P. J. Rauss. "The FERET Evaluation Methodology for Face Recognition Algorithms." *IEEE Trans. on Pattern Analysis and Machine Intelligence*, vol. 22, no. 10, pp. 1090–1104, 2000.
- [41] "The Facial Recognition Technology (FERET) Database." Internet: [http://www.itl.nist.gov/iad/humanid/feret/feret master.html](http://www.itl.nist.gov/iad/humanid/feret/feret%20master.html) [Dec. 10, 2011].
- [42] "The Color FERET Database: Version 2." Internet: <http://www.nist.gov/itl/iad/ig/colorferet.cfm> [Feb. 10, 2012].
- [43] J. Phillips and P. J. Flynn. "Overview of the Face Recognition Grand Challenge." in *Proc. IEEE Conference on Computer Vision and Pattern Recognition*, Jun, 2005.
- [44] P. J. Phillips, P. J. Flynn, T. Scruggs, K. W. Bowyer and W. Worek. "Preliminary Face Recognition Grand Challenge Results." in *Proc. 7th International Conference on Automatic Face and Gesture Recognition*, 2006, pp. 15–24.
- [45] "Face Recognition Grand Challenge (FRGC)." Internet: <http://www.nist.gov/itl/iad/ig/frgc.cfm> [May 8, 2012].
- [46] G. Griffin, A. Holub and P. Perona. "Caltech-256 Object Category Dataset." Tech. Rep., California Institute of Technology, 2007.
- [47] "CalTech 256." Internet: [http://www.vision.caltech.edu/Image\\_Datasets/Caltech256/](http://www.vision.caltech.edu/Image_Datasets/Caltech256/) [Mar. 7, 2012]
- [48] "The Open Source Computer Vision (OpenCV) Library." Internet: <http://opencv.willowgarage.com/wiki/Welcome> [Dec. 16, 2011].
- [49] N. B. Puan and N. Sudha. "A Novel Iris Database Indexing Method Using the Iris Color." in *Proc. 3rd IEEE Conf. on Industrial Electronics and Applications (ICIEA 2008)*, Singapore, Jun 2008, pp. 1886–1891.
- [50] A. Gyaourova and A. Ross. "Index Codes for Multibiometric Pattern Retrieval." *IEEE Trans. on Information Forensics and Security*, vol. 7, no. 2, pp. 518–529, 2012.
- [51] B. Bhanu and X. Tan. "Fingerprint Indexing Based on Novel Features of Minutiae Triplet." *IEEE Trans. on Pattern Analysis and Machine Intelligence*, vol. 25, no. 5, pp. 616–622, 2003.
- [52] R. Cappelli, M. Ferrara and D. Maltoni. "Fingerprint Indexing Based on Minutia Cylinder-Code." *IEEE Trans. on Pattern Analysis and Machine Intelligence*, vol. 33, no. 5, pp. 1051–1057, 2011.
- [53] J. R. Beveridge, D. Bolme, B. A. Draper and M. Teixeira. "The CSU Face Identification Evaluation System." *Machine Vision and Applications*, vol. 16, no. 2, pp. 128–138, 2005.
- [54] S. Arya and D. M. Mount. "Algorithms for Fast Vector Quantization." in *Proc. of DCC '93: Data Compression Conference*, Snowbird, UT, 1993, pp. 381–390.
- [55] S. Arya, D. M. Mount, N. S. Netanyahu, R. Silverman and A. Y. Wu. "An Optimal Algorithm for Approximate Nearest Neighbor Searching in Fixed Dimensions." *Journal of the ACM*, vol. 45, no. 6, pp. 891–923, 1998.

- [56] M. Muja and D. G. Lowe. "Fast Approximate Nearest Neighbors with Automatic Algorithm Configuration." in Proc. International Conference on Computer Vision Theory and Applications (VISAPP'09), 2009, pp. 331–340.
- [57] "FLANN - Fast Library for Approximate Nearest Neighbors." Internet: <http://www.cs.ubc.ca/~mariusm/index.php/FLANN/FLANN> [May 27, 2012].